Spectroscopic ellipsometry study of the $In_{1-x}Ga_xAs_yP_{1-y}$/InP heterojunctions grown by metalorganic chemical-vapor deposition

B. Drevillon and E. Bertran[a)]
Equipe Synthèse de Couches Minces pour l'Energétique, Laboratoire de Physique Nucléaire des Hautes Energies, Ecole Polytechnique, 91128 Palaiseau, France

P. Alnot, J. Olivier, and M. Razeghi
Thomson-CSF, Laboratoire Central de Recherches, Domaine de Corbeville, BP 10, 91401 Orsay, France

(Received 1 April 1986; accepted for publication 31 July 1986)

The dielectric functions of InP, $In_{0.53}Ga_{0.47}As$, and $In_{0.75}Ga_{0.25}As_{0.5}P_{0.5}$ epitaxial layers have been measured using a polarization-modulation spectroscopic ellipsometer in the 1.5 to 5.3 eV region. The oxide removal procedure has been carefully checked by comparing spectroscopic ellipsometry and x-ray photoelectron spectroscopy measurements. These reference data have been used to investigate the structural nature of metalorganic chemical-vapor deposition grown $In_{0.53}Ga_{0.47}As$/InP and $In_{0.75}Ga_{0.25}As_{0.5}P_{0.5}$/InP heterojunctions, currently used for photodiodes and laser diodes. The sharpness of the interfaces has been systematically compared for the two types of heterojunctions: $In_{1-x}Ga_xAs_y$/InP and InP/$In_{1-x}Ga_xAs_yP_{1-y}$. The sharpest interface is obtained for InP growth on $In_{0.75}Ga_{0.25}As_{0.5}P_{0.5}$ where the interface region is estimated to be (10 ± 10) Å thick. The importance of performing *in situ* SE measurements is emphasized.

I. INTRODUCTION

During the past few years, a great deal of attention has been given to superlattices composed of thin layers of differing III-V semiconductors, with the electrons bound in quantum well. The low-pressure metalorganic chemical-vapor deposition (MOCVD) process allows the growth of high quality materials with sharp interfaces.[1-3] The potentially important applications of the quaternary alloys $In_{1-x}Ga_xAs_yP_{1-y}$ lattice matched to InP in the communications industry make them worthy of detailed study.[1] In particular, the InP/InGaAsP/InP double heterostructure lasers operating in the wavelength range 1.2–1.6 μm are attractive light sources for low-loss optical fiber communications. The knowledge of the structure, at the atomic scale, of the interface region between various layers is an important issue of the understanding of the electronic properties of heterojunctions and superlattices. High sensitivity makes spectroscopic ellipsometry (SE) a useful tool for addressing this problem. This has recently been illustrated by an SE investigation of the structural nature of GaAs/GaAlAs and GaAlAs/GaAs heterojunctions.[3]

The present study is devoted to $In_{0.53}Ga_{0.47}As$/InP and $In_{0.75}Ga_{0.25}As_{0.5}P_{0.5}$/InP heterostructures grown by low-pressure MOCVD. The steepness of the heterojunctions will be compared for two types of structures: those produced by the growth of InGaAs (or InGaAsP) on InP and those obtained by the reverse growth sequence. Experimental details concerning the growth procedure, SE, and x-ray photoelectron spectroscopy (XPS) measurements are given in Sec. II. The analysis by SE relies on the knowledge of the dielectric functions of InP, InGaAs, and InGaAsP as discussed in Sec. III. In particular, the oxide removal procedure is systematically studied by comparing SE and XPS measurements. Experiments on the four heterostructures are then discussed in Sec. IV in correlation with the growth mechanisms and the sample preparation procedures.

II. EXPERIMENTAL DETAILS

It has been extensively shown that low-pressure MOCVD is well adapted to the growth of the entire composition range of $In_{1-x}Ga_xAs_yP_{1-y}$ alloys lattice matched to InP from $y = 0$ (InP) to $y = 1$ ($In_{0.53}Ga_{0.47}As$)[1]. Two types of heterojunctions are considered in this paper: $In_{0.53}Ga_{0.47}As$/InP[4] and $In_{0.75}Ga_{0.25}As_{0.5}P_{0.5}$/InP.[5] The growths were carried out at 76 Torr, at substrate temperatures of 550 °C (InGaAs/InP) and 650 °C (InGaAsP/InP) with the following deposition rates: 100 Å mn^{-1} (InP), 200 Å mn^{-1} (InGaAs), and 140 Å mn^{-1} (InGaAsP). The heterostructures are obtained by depositing a 70-Å-thick epilayer on top of the corresponding substrate. This thickness was chosen in order to enable SE measurements to be sensitive to the interface region. However, a different growth procedure is used when producing quantum-well structures.[1] Before exposure to air, in order to prevent As and/or P effusion, the heterostructures were cooled in the deposition reactor under a gaseous atmosphere which depends on the nature of the top layer of the sample. The following gases were used: PH_3 (InP as top layer), AsH_3 (InGaAs as top layer), and a (AsH_3,PH_3) mixture (InGaAsP as top layer). Further experimental details can be found in Ref. 1.

The spectroscopic ellipsometer is a polarization-modulation type described in detail elsewhere.[6] The spectral range of this instrument is 1.5 to 5.3 eV, SE data being regularly recorded with an 0.05 eV interval. Let us recall that SE measures, as a function of the energy, the complex reflectance ratio:

$$\rho = R_p R_s^{-1} = \tan \psi \exp(i\Delta) , \quad (1)$$

[a)] Present address: Laboratori de Capes Primes, Facultat de Fisica, Universitat de Barcelona, Av. Diagonal, 645, 08028 Barcelona, Spain.

Downloaded 14 Jun 2010 to 161.116.168.169. Redistribution subject to AIP license or copyright; see http://jap.aip.org/jap/copyright.jsp

between the reflection coefficient R_p and R_s for a linearly polarized light with its polarization, respectively, parallel and perpendicular to the plane of incidence. In the case of a bulk material with a sharp interface with ambient, ρ is directly related to the dielectric function $\epsilon(E)$ of the material through the relationship:

$$\epsilon(E) = \epsilon_1 - i\epsilon_2 = \sin^2\theta\left[\mathrm{tg}^2\theta\left(\frac{1-\rho}{1+\rho}\right)^2 + 1\right], \quad (2)$$

where θ is the angle of incidence of the light on the sample. Chemical treatments of the samples, prior to SE measurements, were performed by flowing solutions over the vertical surface of an optically prealigned substrate, then maintaining the sample in a dry N_2 flow while taking SE data in order to prevent a native oxide growth.

The XPS data were recorded using an ESCALAB MARK II apparatus using Al$K\alpha$ radiation. Calibration of XPS spectra has been performed assuming the hydrocarbon peak to be at 285.0 eV. Etching of substrate, prior to XPS measurements, has been performed under nitrogen atmosphere inside a glove box. Freshly etched samples were fed into the XPS apparatus from the glove box, using an hermetic vessel kept under nitrogen atmosphere. Through this procedure etched samples were never in contact with air before XPS characterization.

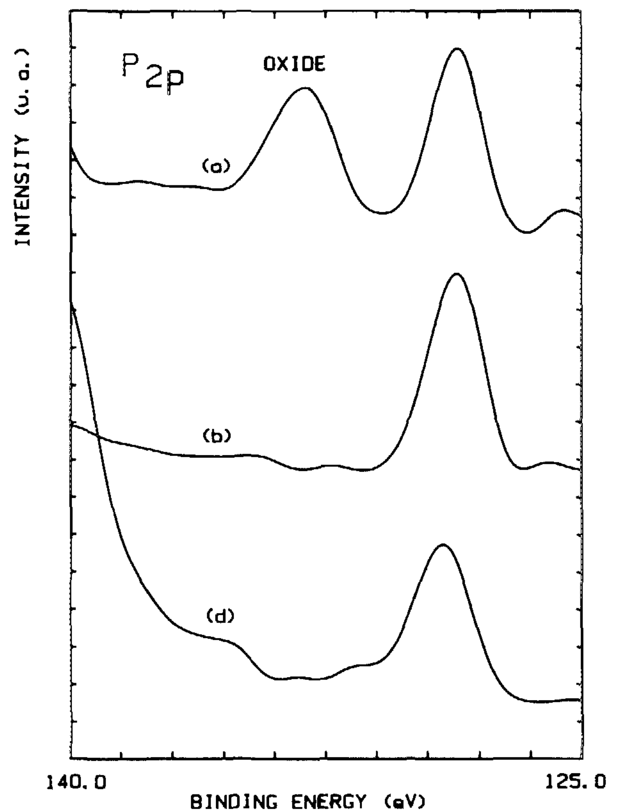

FIG. 1. P($2p$) core level peak recorded for; (a) air-oxidized InP and (b) and (d) etched HF:H_2O (1:10) InP and InGaAsP samples.

III. REFERENCE DIELECTRIC FUNCTIONS

As already mentioned, the SE study of the heterojunctions needs the knowledge of the dielectric functions of the bulk InP, $In_{0.53}Ga_{0.47}As$, and $In_{0.75}Ga_{0.25}As_{0.5}P_{0.5}$ materials. However, the corresponding $\epsilon(E)$ functions cannot be deduced directly from SE measurements using Eq. (2) because of the presence of a native oxide surface layer. It has been shown that SE provides an highly sensitive indication of the sharpness of the dielectric discontinuity between substrate and ambient.[7] Different chemical etching and cleaning procedures were compared by XPS and SE measurements. The SE measurements were performed, in a dry N_2 flow, immediately afterwards. XPS measurements revealed that this procedure prevents a native oxide growth. Best results were obtained by using a (1:10) solution of HF: deionized H_2O. However, it has been shown in the case of [100] GaAs surfaces that acid solutions can produce deep microroughness.[8] These effects are illustrated by comparing SE and XPS measurements.

The XPS measurements are shown in Figs. 1–4. Core levels and Auger lines P($2p$), In($3d$ 5/2), As (Auger LMM), and Ga (Auger LMM) have been recorded. In order to observe the oxide removal from InP, InGaAs, and InGaAsP surfaces, it is important to know the binding energies of the core levels and the kinetic energies of the Auger lines corresponding to the elements In, As, Ga, and P in their oxidized forms or in the III-V compounds. GaAs and InP, because they have been extensively studied, have been chosen as reference samples. Spectra shown in Figs. 1(a)–4(a), correspond to air-oxidized InP and GaAs samples which have been chemically etched prior to air exposure. Concerning P($2p$), Ga, and As(Auger), oxide components are clearly visible in all XPS spectra. This is less clear concerning

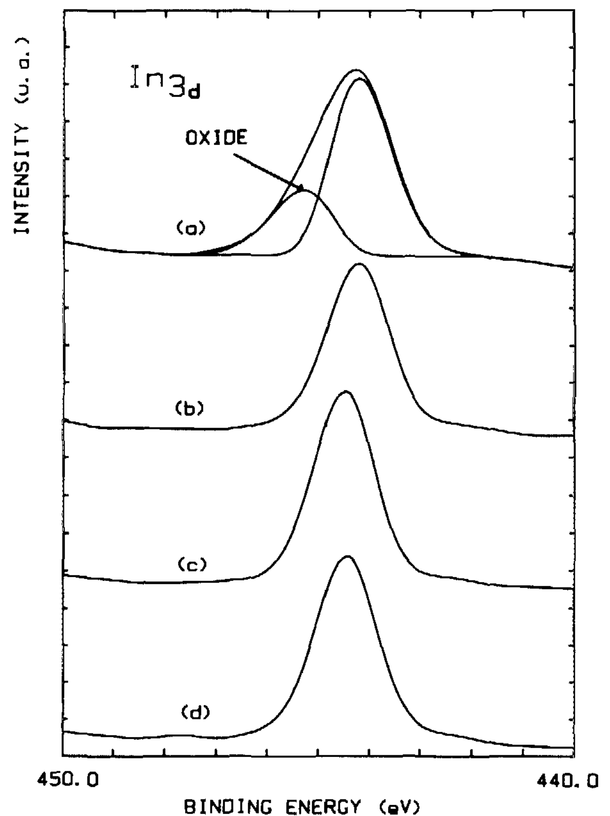

FIG. 2. In($3d$) core level peak recorded for; (a) air-oxidized InP and for etched HF:H_2O (1:10) samples; (b) InP, (c) InGaAs, (d) InGaAsP.

Downloaded 14 Jun 2010 to 161.116.168.169. Redistribution subject to AIP license or copyright; see http://jap.aip.org/jap/copyright.jsp

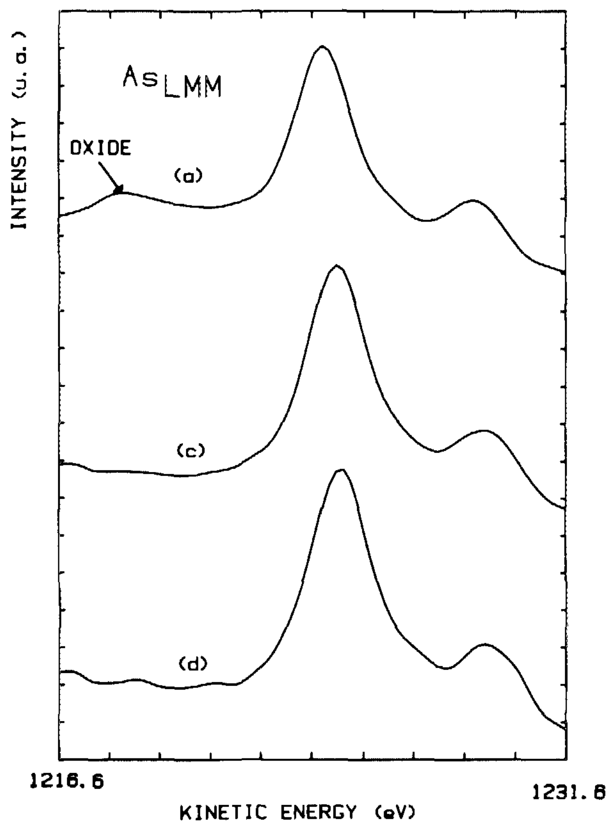

FIG. 3. As(LMM) Auger lines recorded for; (a) air-oxidized GaAs and for etched HF:H_2O (1:10) samples; (c) InGaAs, (d) InGaAsP.

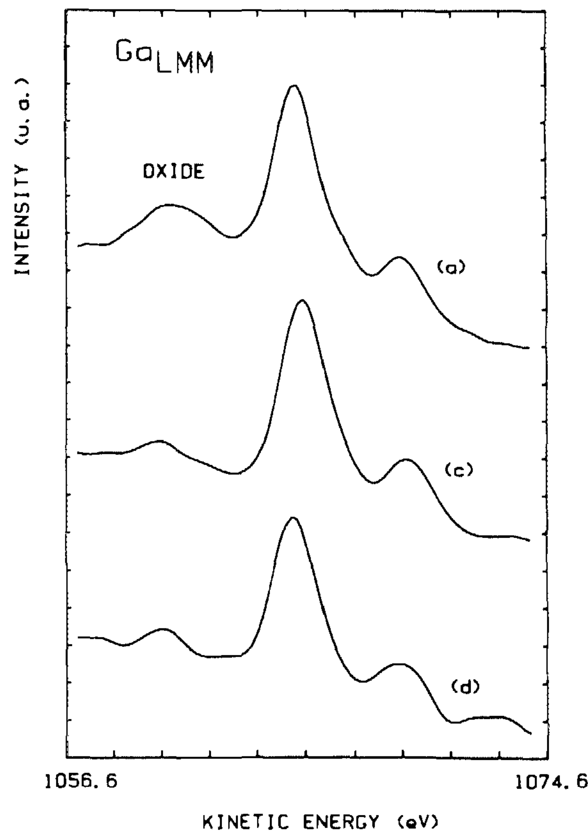

FIG. 4. Ga(LMM) Auger lines recorded for; (a) air-oxidized GaAs and for etched HF:H_2O(1:10) samples; (c) InGaAs, (d) InGaAsP.

In(3d) due to small chemical shifts existing between, indium in InP: binding energy (BE) = 444.4 eV and indium in In_2O_3: BE = 444.7 eV or $In(OH)_3$: BE = 445.3 eV.[9] As a matter of fact, In core level has been fitted with Gaussians in order to evidence the oxide component [see Fig. 2(a)]. XPS data were then taken after performing the HF (1:10) etching treatment on three different air-oxidized substrates: InP, InGaAs, and InGaAsP (Figs. 1–4). We can notice that the components characteristic of overlayer oxide have disappeared from all XPS spectra, inferring oxide removal due to the etching treatment.[10,11] All these results are in agreement with previous analysis, which have also shown the efficiency of HF etching solution in performing oxide removal.[12,13] Immersion times from 1 s to 1 min in the etching solution did not produce any modification in the XPS spectra.

The SE measurements corresponding to the extreme values of y (InP and $In_{0.53}Ga_{0.47}As$) are presented in Fig. 5. In order to interpret the data displayed in this figure, let us recall that the presence of an oxide layer and/or a surface microroughness both induce a decrease of the ϵ_2 spectra (together with a shift to lower energies), these effects being more sensitive in the 4.5-eV region (E_2 peak).[7,8,12] The first chemical treatment (solid lines) performed by flowing the solution for 1 s over the surface results in an increase of E_2 peak which corresponds to the oxide removal, as evidenced

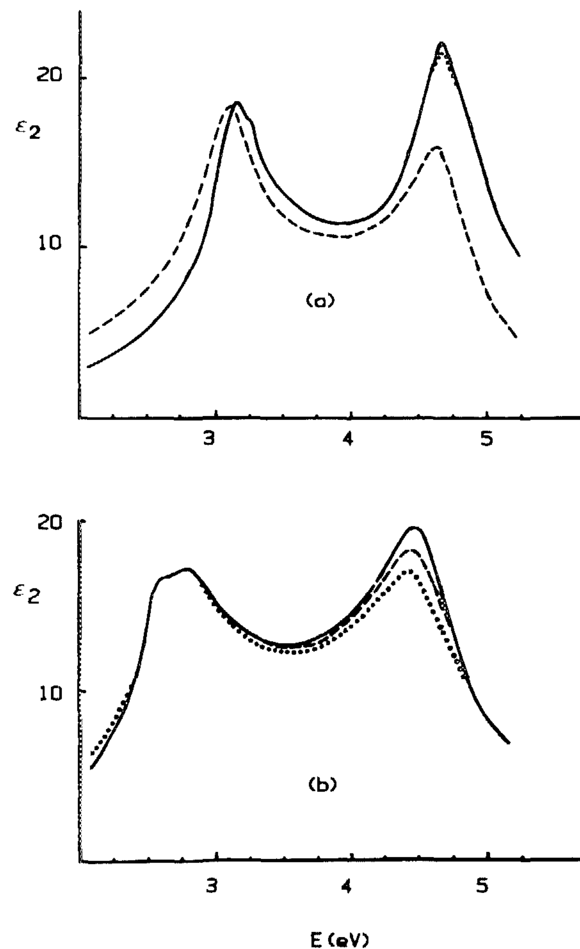

FIG. 5. Influence of the (1:10) HF solution etching on the pseudodielectric function of InP (a) and $In_{0.53}Ga_{0.47}As$(b); dashed lines: as-deposited samples, solid lines: 1-s treatment, dotted lines: 3 s treatment.

Downloaded 14 Jun 2010 to 161.116.168.169. Redistribution subject to AIP license or copyright; see http://jap.aip.org/jap/copyright.jsp

by the XPS measurements. However, an extension of this chemical treatment for more than 1 s produces a decrease of the E_2 peak revealed by SE measurements (Fig. 5: dotted lines) which can be correlated with the presence of a surface microroughness. In conclusion, the 1 s treatment by the HF solution was then systematically applied to each sample before SE measurements.

Real and imaginary parts, $\epsilon_1(E)$ and $\epsilon_2(E)$, of the complex dielectric functions of the three reference materials are shown in Fig. 6. The two major features of the spectra are the E_1 and E_2 structures at 3 and 4.5 eV, respectively. More precisely, all of the ϵ_2 spectra displayed in Fig. 6 have two features in the E_1 structure corresponding to the E_1 and $E_1 + \Delta_1$ transitions between the spin-orbit-split upper valence band and the lowest conduction band along the [111] direction in the Brillouin zone. Detailed information about interband critical points of $In_{1-x}Ga_xAs_yP_{1-y}$ alloys are given elsewhere.[15] The three ϵ_1 (or ϵ_2) spectra are clearly distinguishable, the E_1 and E_2 structures move to lower energies with increasing y from $y = 0$ (InP) to $y = 1$ ($In_{0.53}Ga_{0.47}As$). The data displayed in Fig. 6 can be compared to previous measurements obtained with a rotating analyzer ellipsometer (RAE)[14] on InGaAsP samples grown by liquid-phase epitaxy. The overall agreement is rather good. However, the dominant E_2 peaks in $\epsilon_2(E)$ are 2–5% higher in Kelso *et al.*[15] measurements but are 10% lower in E_1 region (~ 3.0 eV). The weak discrepancy in the E_2 region can be possibly attributed to differences in sample growth and surface preparation. As a matter of fact we have checked that a 5-Å-thick In_2O_3 overlayer, or a very small surface microroughness (5-Å-thick overlayer with 50% density deficiency) can account for the observed discrepancy in InP near 4.5 eV. But more generally, differences in $\epsilon_2(E)$ data can reflect differences in the measurement procedures. In particular, it can be noticed that the RAE measures $\cos\Delta$ [as defined by Eq. (1)] whereas the polarization modulation ellipsometer measures either $\cos\Delta$ or $\sin\Delta$. Therefore, as already pointed out,[16] the RAE will be at a disadvantage when attempting to measure materials where Δ is close to 0° (or 180°), such as $In_{1-x}Ga_xAs_yP_{1-y}$ (from $y = 0$ to $y = 1$) in the E_1 region.

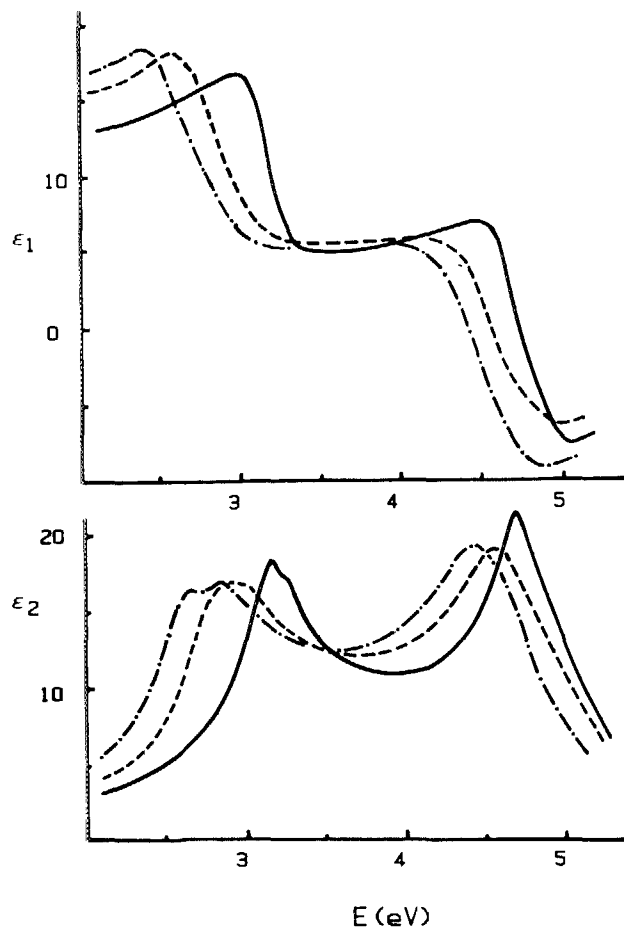

FIG. 6. Real parts and imaginary parts ($\epsilon_1\epsilon_2$) of dielectric function spectra of InP (solid lines), $In_{0.53}Ga_{0.47}As$ (dashed–dotted lines) and $In_{0.75}Ga_{0.25}As_{0.5}P_{0.5}$ (dashed lines).

IV. EXPERIMENTAL RESULTS AND DISCUSSION

Four samples of heterostructures have been examined:

(a) A 70-Å $In_{0.53}Ga_{0.47}As$ epilayer on an InP substrate.

(b) A 70-Å InP epilayer on an $In_{0.53}Ga_{0.47}As$ thick layer (2000 Å) grown on an InP substrate.

(c) A 70-Å $In_{0.75}Ga_{0.25}As_{0.5}P_{0.5}$ epilayer on an InP substrate.

(d) A 70-Å InP epilayer on an $In_{0.75}Ga_{0.25}As_{0.5}P_{0.5}$ thick layer (2000 Å) grown on an InP substrate.

In each case, the cleaning procedure described above was applied before SE measurements. The $\epsilon(E)$ functions of the heterostructures, given in Fig. 7, clearly differ from the data of Fig. 6 which correspond to the bulk materials. Because of the thin thickness of the epilayer (70 Å), the optical response of the substrates clearly influences the SE measurements displayed in Fig. 7, this effect being more sensitive in the E_1 region (~ 3.0 eV). In order to detect the presence of an interface region between the substrate and the epilayer, the experimental $\epsilon_2(E)$ measurements have been compared in Fig. 8 to a calculation using the reference dielectric functions shown in Fig. 6 and assuming a sharp interface between the substrate and a 60 Å (dotted lines) or 80 Å (dashed lines) overlayer. The experimental ϵ_2 curves only interpolate both calculations in Fig. 8(d) (InP/InGaAsP). In contrast, in Figs. 8(a), (b), and (c) the experimental curves clearly depart from the calculations in the E_2 region, showing the influence of a transition region in those cases.

This interface region may be tentatively described by assuming that the substrate and the epilayer are mixed inside a very thin layer without changing their chemical nature.[3] Such a physical mixture simulates a rough interface at the atomic scale between the substrate and the epilayer. The dielectric function of the interface layer is computed using the standard effective medium approximation.[17] A least-square fit of the data displayed in Fig. 7 is then performed, the free parameters of the fit being: f_s, the volume fraction of the substrate inside the interface layer; d_0 and $d_{\rm int}$, the thicknesses of the epilayer and the interface layer, respectively. In order to perform quantitative comparisons between the four heterostructures, the values of the fit residual $\delta^2_{\rm min}$, defined as the minimum of:

$$\delta^2 = \frac{1}{N}\sum_{i=1}^{N} |\epsilon_{\rm exp}(E_i) - \epsilon_{\rm calc}(E_i, f_s, d_{\rm int}, d_0)|^2$$

Downloaded 14 Jun 2010 to 161.116.168.169. Redistribution subject to AIP license or copyright; see http://jap.aip.org/jap/copyright.jsp

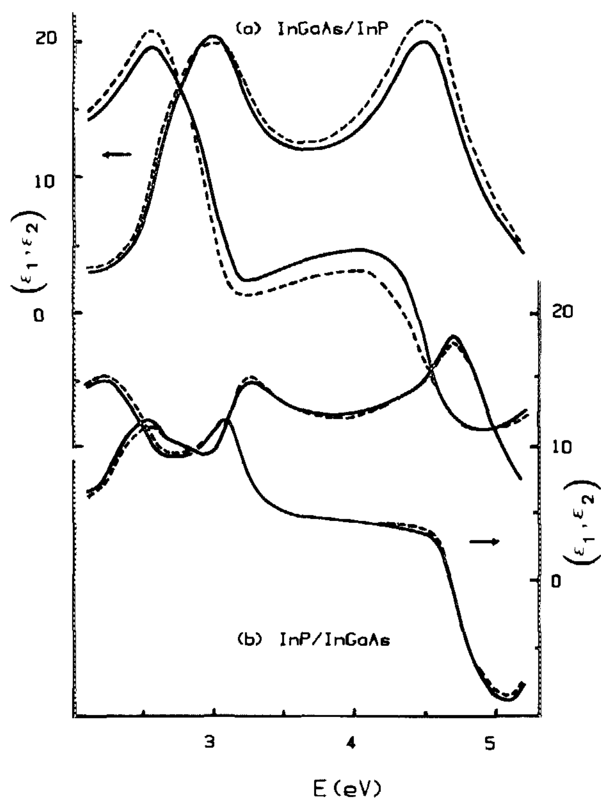

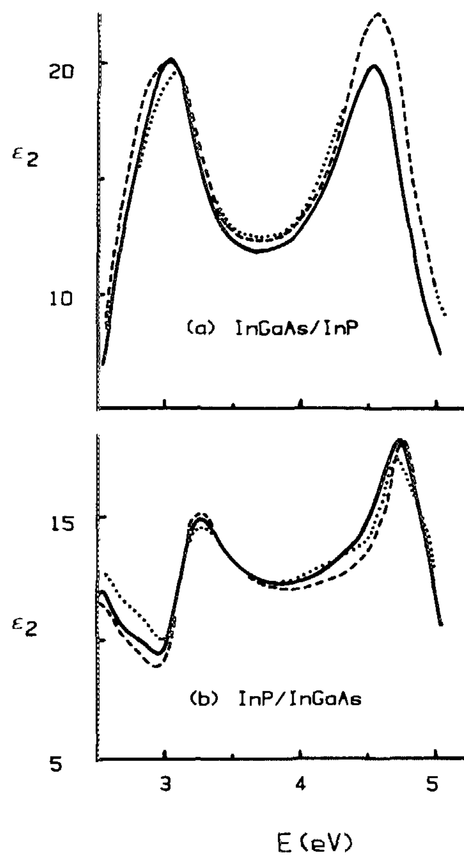

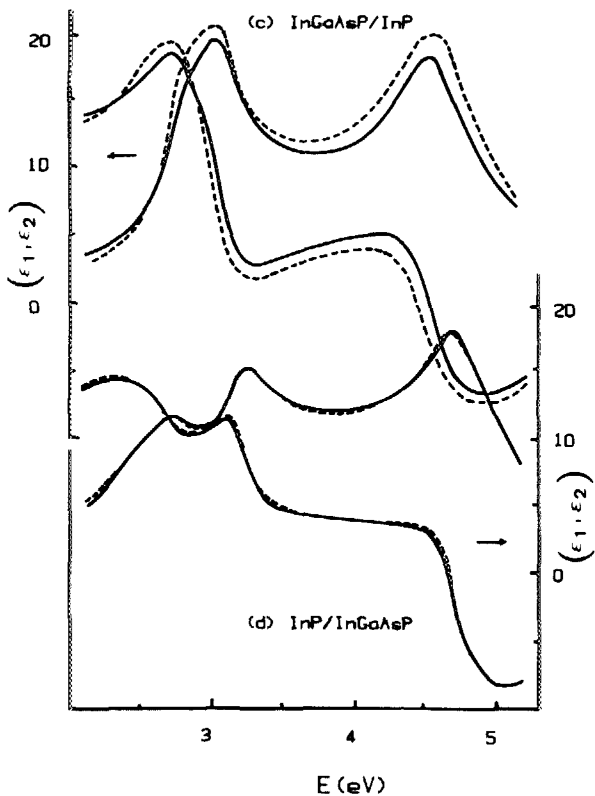

FIG. 7. Experiment (solid lines) and best fit to the data (dashed lines) using the physical interface model of the heterostructures.

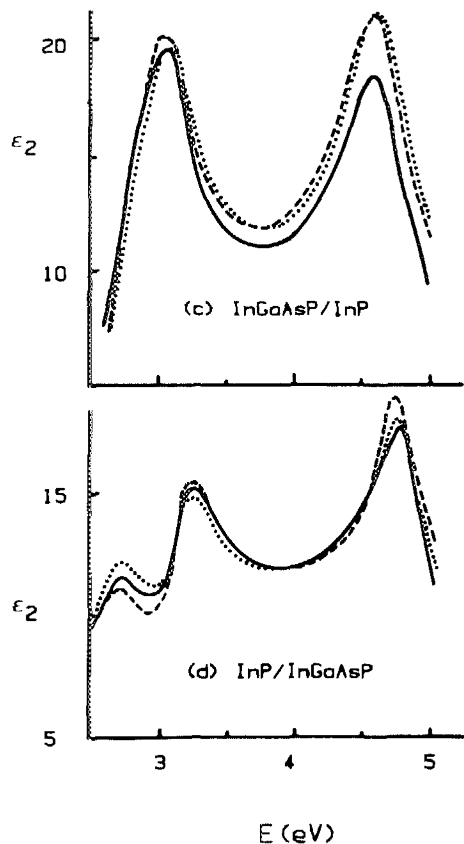

FIG. 8. Experiment (solid lines) and modelings (dotted and dashed lines: 60- and 80-Å-thick epilayers) assuming a sharp interface of the heterostructures.

(where N is the number of experimental measurements) regularly performed at energies E_i with $\Delta E_i = 0.05$ eV, are compared in Table I. The results of the fits are compared to the experimental $\epsilon(E)$ curves in Fig. 7 (dashed lines). Best matches between calculated and experimental curves are ob-

Downloaded 14 Jun 2010 to 161.116.168.169. Redistribution subject to AIP license or copyright; see http://jap.aip.org/jap/copyright.jsp

TABLE I. Results of the fit to the physical interface model.

Sample	Type	δ^2_{min}
a	InGaAs/InP	3.0
b	InP/InGaAs	0.1
c	InGaAsP/InP	6.0
d	InP/InGaAsP	0.2

tained for samples b and d (InP epilayer). In contrast, δ^2_{min} increases by a factor of 30 when using the reverse growth sequences (InP substrate). In particular in these later cases, the physical interface model fails to reproduce the $\epsilon_2(E)$ data in the E_2 region [see Figs. 7(a) and 7(c)].

Let us discuss first the cases corresponding to InP epilayer (samples b and d). The values of the fitted parameters obtained with these samples are displayed in Fig. 9. It can be noticed that the overall thickness value ($d_{int} + d_0$) obtained using the physical interface model is in very good agreement with the expected epilayer thickness (70 Å). The precision on the fitted parameters values can be estimated by varying the spectral range of the dielectric function used in the fit. The following typical values were obtained ± 0.1 on f_s and ± 10 Å on d_{int} and d_0. In each case a small interface layer is obtained whose physical composition is closed to InP ($f_s \sim 0.80$). However, the sharpest interface is obtained by depositing InP on InGaAsP (sample d), in this case the existence of an interface layer is not evidenced ($d_{int} = 10 \pm 10$ Å). The dielectric functions of both interface layers can be estimated by using the fitted values of f_s. The corresponding imaginary parts of the dielectric functions are compared to InP in Fig. 10. As expected, the optical responses of the interface layers of samples b and d are found to be very close to InP. This leads to two possible interpretations. First, a rough interface is produced in the sample b but the difference between both samples b and d revealed by the physical interface model (see Fig. 9) remains unclear. Second, there is an interdiffusion between the substrate and the epilayer (InP) leading to a formation of a thin layer of a quaternary alloy with a chemical nature different from the substrate. In this

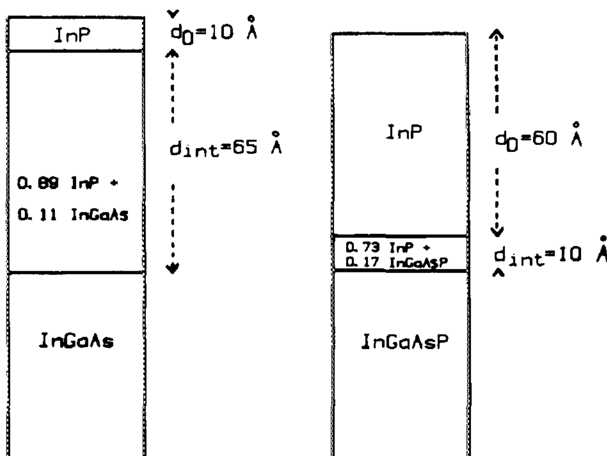

FIG. 9. Structures of heterojunctions (InP epilayer) as determined by using the physical interface model.

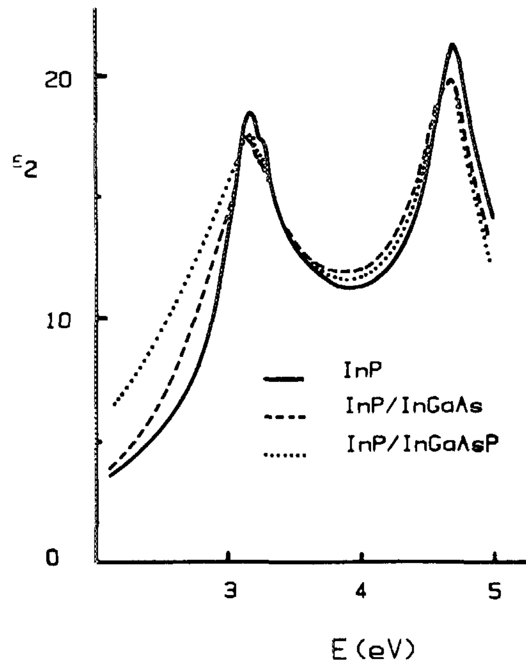

FIG. 10. Determination of the imaginary part of the dielectric function of the interface layers (InP epilayer) using the physical interface model, compared to InP.

frame, the results displayed in Fig. 10 can be understood as an estimation of the optical response of the interface layer. An inspection of Fig. 10 shows that the composition of this quaternary alloy $In_{1-x}Ga_xAs_yP_{1-y}$ is probably close to $y = 0$ (InP). Moreover, with this latter chemical interface model a sharper interface is expected in sample d in which the underlayer is already a quaternary alloy ($In_{0.75}Ga_{0.25}As_{0.5}P_{0.5}$), than in sample b (substrate InGaAs). Indeed, the difference between sample b and d, revealed by the physical interface model can be correlated to the growth conditions. In both cases before the growth of the InP layer, the introduction of $Ga(C_2H_5)_3$ and AsH_3 is interrupted but the phosphine remains present in the reactor only in the case of the deposition of InP on InGaAsP (sample d). Then, the difference between both interfaces can reflect the diffusion time of the phosphorous toward the neighborhood of the growth surface in the case of InP/InGaAs (sample b). This interpretation has been recently confirmed by an Auger analysis taken along a chemically bevelled quantum-well InP/InGaAs/InP.[18]

Let us now consider the opposite cases in which InP is the substrate (samples a and c). The results of Table I show that in both cases a very bad agreement with the physical interface model is obtained. This may be attributed to the presence of a large chemical interface. However, results from Auger spectra of a chemically etched bevel through $Ga_{0.47}In_{0.53}$As-InP quantum wells do not seem to support this hypothesis.[18] But it has to be noticed that the quantum-well structures are produced using a different growth procedure. In this later case, the ternary layer is located between InP epitaxial layers. Furthermore, the only spectral region of Figs. 7(a) and 7(c) where chemical interface would play a significant role is the vicinity of E_1 transitions. If a chemical mixing were present the corresponding peak would be

Downloaded 14 Jun 2010 to 161.116.168.169. Redistribution subject to AIP license or copyright; see http://jap.aip.org/jap/copyright.jsp

substantially broadened, which it is not. Likewise, chemical mixing could not possibly lower the value of the E_2 peak in ϵ_2 nor raise the value of ϵ_1. So, we favor another interpretation. Obviously, the optical response of the thin 70-Å-thick epilayers (InGaAs and InGaAsP) are incompatible with the corresponding bulk dielectric functions obtained by using 2000-Å-thick InGaAs and InGaAsP grown on InP, as shown in Fig. 6. These differences may possibly reflect differences in sample preparation. In particular, let us recall that during the cooling procedure in the deposition reactor before SE measurements, the introduction of group III-alkyls is interrupted in both cases, group V hydrides being still resident in the reaction tube. Then, the composition of the gaseous boundary layer is expected to vary in the early stage of the cooling procedure, before complete evacuation of the groups III-alkyls. However, the epitaxial growth is controlled by the mass transport of group III species.[1] This can result in a modification of the composition of the InGaAsP epilayer near the surface. Furthermore, the gaseous composition inside the deposition reactor being fixed, the chemical nature of the $In_{1-x}Ga_xAs_yP_{1-y}$ alloys is known to vary as a function of the substrate temperature. Then the deposited InGaAs or InGaAsP material in these conditions may be polycrystalline, resulting in a lowering of the E_2 peak in ϵ_2 observed in Figs. 7(a) and 7(c). The influence of these effects on the optical response of the sample is expected to be relatively stronger for a thin overlayer (70 Å) than for the bulk InGaAs or InGaAsP. Because of the high stability as a function of the substrate temperature of the InP layer, this discrepancy between the dielectric functions of a thin epilayer and bulk material is not observed in samples b and d (InP epilayer).

Obviously, *in-situ* ellipsometric measurements have to be performed in real time to check these hypothesis. First, spectroscopic ellipsometry appear to be a valuable tool to measure *in situ* the chemical nature variation of the $In_{1-x}Ga_xAs_yP_{1-y}$ alloys during the cooling procedure in the deposition chamber. And second, real time measurements at a fixed wavelength by kinetic ellipsometry are known to be very sensitive to the early stage of the growth at the atomic scale.[19] This technique appears to be well adapted to perform high precision studies of the interface region.

V. CONCLUSION

It has been shown that polarization-modulation spectroscopic ellipsometry is well adapted for a detailed study of the InGaAs/InP and InGaAsP/InP heterostructures. The steepness of the heterojunctions has been compared for two types of structures: those produced by the growth of InGaAs (or InGaAsP) on InP and those obtained by the reverse growth sequence. Sharpest interface is obtained for InP growth on $In_{0.75}Ga_{0.25}As_{0.5}P_{0.5}$ where the interface region is estimated to be (10 ± 10) Å thick. This clearly shows that very sharp interfaces can be grown by MOCVD. This result confirms similar conclusions obtained on GaAlAs/GaAs heterostructures.[3] The importance of performing *in situ* and real time measurements has been emphasized. A more accurate characterization of these interfaces by *in-situ* SE is planned.

ACKNOWLEDGMENTS

One of the authors, E. Bertran is kindly endebted to CIRIT of Generalitat de Catalunya for his support. We also thank Dr. J. P. Duchemin and A. Friederich for interest and support and A. M. Antoine for contribution in data modeling.

[1]M. Razeghi, *Semiconductors and Semimetals*, Vol. 22, part A, edited by T. W. Tsang (Academic, New York, 1985), p. 299.
[2]M. J. Ludowise, J. Appl. Phys. **58**, R31 (1985).
[3]M. Erman, J. B. Theeten, N. Vodjdani, and Y. Demay, J. Vac. Sci. Technol. B **1**, 328 (1983).
[4]Y. Guldner, J. P. Vieren, P. Voisin, M. Voos, M. Razeghi, and M. A. Poisson, Appl. Phys. Lett. **40**, 877 (1982).
[5]M. Razeghi and J. P. Duchemin, J. Cryst. Growth **70**, 145 (1984).
[6]B. Drevillon, J. Perrin, R. Marbot, A. Violet, and J. L. Dalby, Rev. Sci. Instrum. **53**, 969 (1982).
[7]D. E. Aspnes, J. Vac. Sci. Technol. **17**, 1057 (1980).
[8]D. E. Aspnes and A. A. Studna, Appl. Phys. Lett. **46**, 1071 (1985).
[9]G. Hollinger, E. Gergignal, J. Joseph, and Y. Robach, J. Vac. Sci. Technol. A **3**, 2082 (1985).
[10]The weak Ga peaks at energies 1060 eV shown in Figs. 4(c) and (d) are attributed to Auger satellite peaks of unoxidized Ga in InGaAs or InGaAsP (see Ref. 11).
[11]E. Antonides, E. C. Janse, and G. A. Sawatzky, Phys. Rev. B **15**, 4596 (1977).
[12]A. Guilvarc'h, H. L'haridon, G. Peloris, G. Hollinger, and P. Pertosa, J. Appl. Phys. **55**, 55 (1984).
[13]S. K. Krawczik and G. Hollinger, Appl. Phys. Lett. **45**, 871 (1984).
[14]S. M. Kelso, D. E. Aspnes, M. A. Pollack, and R. E. Nahory, Phys. Rev. B **26**, 6669 (1982).
[15]B. Drevillon and F. Vaillant, Thin Solid Films **124**, 217 (1985).
[16]G. E. Jellison and F. A. Modine, J. Appl. Phys. **53**, 3745 (1982).
[17]D. A. G. Bruggeman, Ann. Phys. (Leipzig) **24**, 636 (1935).
[18]P. Alnot, A. Huber, and J. Olivier, Surf. Interface Anal. **9**, 283 (1986).
[19]B. Drevillon, Thin Solid Films, **130**, 165 (1985).

Downloaded 14 Jun 2010 to 161.116.168.169. Redistribution subject to AIP license or copyright; see http://jap.aip.org/jap/copyright.jsp